International Information and Engineering Technology Association
Advancing the World of Information and Engineering

Comparative Numerical Analysis of Torpedo-Shaped and Cubic Symmetrical Autonomous Underwater Vehicles in the Context of Indonesian Marine Environments

Kadek Dwi Wahyuadnyana[1,2*] , Katherin Indriawati[1] , Purwadi Agus Darwito[1] , Ardyas Nur Aufa[2] , Hilton Tnunay[2,3]

[1] Department of Engineering Physics, Sepuluh Nopember Institute of Technology (ITS), Surabaya 60111, Indonesia
[2] Control and Navigation Group, Research Department, Beehive Drones, Yogyakarta 55582, Indonesia
[3] Department of Civil Engineering, Faculty of Engineering Technology, KU Leuven, Geomatics, 9000 Ghent, Belgium

Corresponding Author Email: katherin@ep.its.ac.id

ABSTRACT

This study presents a comparative analysis of the performance dynamics of torpedo-shaped and cubic symmetrical autonomous underwater vehicles (AUVs) within the unique context of Indonesian marine environments. The dynamics of these AUV models were assessed in MATLAB's ode45 solver, incorporating real-world sea wave data from Indonesian waters as external disturbance variables. As the AUVs were subjected to these disturbances, the performance of each model's positional capability was critically evaluated to determine their respective hydrodynamic attributes. Notably, the cubic symmetrical AUV model demonstrated superior trajectory following and differential actuation capabilities, indicating its aptness for missions necessitating meticulous path-tracking. Conversely, the torpedo-shaped AUV showcased an enhanced robustness in managing external disturbances, particularly when viewed from a bi-dimensional standpoint. The selection between these AUV models is contingent upon the specific mission requirements, including environmental factors, mission objectives, and design capabilities. This comparative investigation offers valuable insights into the design and operation of AUVs in the Indonesian marine environment, thus informing the development of optimized AUV models tailored to tackle the unique challenges of this maritime context. The findings from this study contribute significantly to the progression of underwater exploration, environmental surveillance, and offshore industries operating within Indonesian waters.

1. INTRODUCTION

Occupying a strategic position between the Pacific and Indian Oceans, Indonesia boasts a maritime territory of 6.4 million km^2 [1] and a coastline stretching over 81 thousand km [2]. Despite this extensive maritime domain, underwater exploration within Indonesian waters remains underdeveloped. As such, a wealth of possibilities related to marine life, biodiversity, and resource discovery remain largely unexplored. Numerous factors contribute to this situation, with the challenging conditions of the Indonesian seas presenting significant obstacles to exploration and the advancement of underwater technology. Thus, it is a matter of urgency to conduct comprehensive research that aligns the development of underwater technology with the unique conditions and characteristics of the Indonesian sea.

Research has indicated that ocean wave characteristics in Indonesian waters are heavily influenced by monsoon winds and ocean currents [3]. Short-period waves predominantly occur within the inner Indonesian seas, while long-period waves are more common in outer seas [4]. A study conducted by Rachmayani et al. [5] calculated calm water period data by summing the number of months when wave height nearest to sub-districts was less than 0.5m. Further research by Rachmayani et al. [6] sought to understand ocean wave characteristics and identify periods and areas susceptible to high waves in Indonesian waters, utilizing the significant wave height of the Windwaves-05 model for analysis in the Western Indonesian Seas. Additionally, a study by Anggraini et al. [7] drew data from various Indonesian seas, including average wave height, wave period, and wavelength, to analyze the energy potential of Indonesian ocean waves using an oscillating water column energy converter. This research encompassed approximately 15 seas in Indonesia and revealed significant variations in the state of Indonesian seas. These variations, influenced by geographical location and oceanic surroundings, present considerable challenges to underwater exploration.

Autonomous Underwater Vehicles (AUVs) are critical for various underwater applications, including ocean exploration [8-10], environmental monitoring [11, 12], and underwater surveys [13, 14]. The hydrodynamic characteristics and performance of AUVs significantly influence their maneuverability, efficiency, and stability. Several physical

AUV models exist, such as the torpedo-like model [15], the cubic symmetrical model [16], and biomimetic models [17] that mimic the shape of undersea creatures. However, the implementation of biomimetic models remains challenging due to material limitations and nonlinearity, making the torpedo-like and cubic symmetrical models preferred choices for underwater research or exploration. The selection of an AUV's physical model is vital, as it affects performance, maneuverability, and adaptability to diverse marine conditions. Effective design can enhance movement efficiency and ensure stable navigation across various sea states. Therefore, the choice of the appropriate physical model is crucial for the development of reliable and efficient underwater vehicles suitable for a range of missions.

Regrettably, there is a dearth of studies considering the selection of physical models of AUVs, particularly the torpedo-like or cubic symmetrical models, in relation to the specific conditions of Indonesian waters. The primary objective of this study, therefore, is to examine and evaluate the dynamic response of both AUV models concerning the conditions of Indonesian waters. It aims to propose an AUV model optimally suited for underwater exploration missions in Indonesian waters.

Several research studies focus on the cubic symmetrical AUV model, with its dynamic equations extensively explored and obtained in references [18, 19]. These studies employ the global reference frame and body-frame coordinates to represent their cubic symmetrical AUV model, considering it a six degrees of freedom (6 DoF) system, which includes linear locations in the X, Y, and Z axes and angular positions in the roll, pitch, and yaw directions.

Conversely, Wahed and Arshad [20] proposed a mathematical model of a torpedo-like AUV, named μAUV (micro-AUV), which disregards the effects of the lift force on the AUV. The mathematical model for the control law was created using theoretical and empirical techniques adapted from similar AUVs, and the SolidWorks 3D model data was employed to determine the AUV's parameters. The equations of motion for the Torpedo-Like AUV model were then derived in relation to the characteristics previously examined in references [21, 22].

Given the body of research conducted on both AUV models, it is advantageous to analyze the dynamic response of each AUV model to the characteristics of the Indonesian sea. In this study, a comparative numerical simulation of a torpedo-like and a cubic symmetrical AUV design is presented, set within the challenging marine environments of Indonesia. The aim is to analyze the hydrodynamic performance of these models in Indonesian waters to understand their suitability for specific tasks and conditions. This study will provide valuable insights into the design and operation of AUVs in Indonesian waters by comparing torpedo-like and cubic symmetrical AUV models. By identifying optimal design features for efficient and stable maneuvering, this research can contribute to the development of AUVs tailored to Indonesian marine environments, benefiting underwater exploration, environmental monitoring, and offshore industries.

2. AUV MODEL DYNAMICS

2.1 Cubic symmetrical AUV model

The chosen cubic symmetrical AUV model used in this paper is based on the ROV model by Blue Robotics [23]. Previous studies [16], Li et al. [18] have extensively investigated and derived this model's dynamic equations. The authors present this cubic symmetrical AUV model in two coordinate frames: the global reference and body-frame coordinates. This model is considered to have six degrees of freedom (6 DoF), encompassing angular positions: roll (ϕ), pitch (θ), yaw (ψ), and linear positions: in the x, y, and Z axes. Figure 1 illustrates the representation of the cubic symmetrical AUV model, including the global reference and the body-frame coordinates.
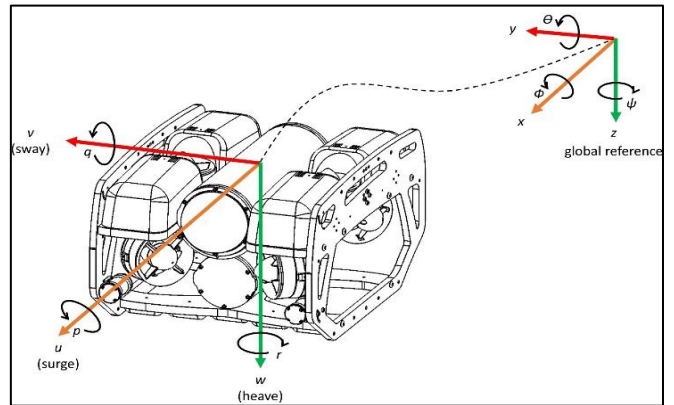
Figure 1. Physical model and the reference frames for cubic symmetrical AUV motion

Eq. (1) gives the dynamic equation of motion of general AUV based on [24]:

$$M\dot{v} + C(v)v + D(v)v + g(\eta) = \tau + w. \tag{1}$$

Based on Eq. (1), M is the inertia matrix, where $M_{\dot{u}} = m - X_{\dot{u}}$, $M_{\dot{v}} = m - Y_{\dot{v}}$, and $M_{\dot{r}} = I_z - N_{\dot{r}}$ are the inertia terms including added mass, which represents the additional virtual mass that the AUV experiences due to the displacement of water as it moves; $C(v)$ is the Coriolis, and centripetal matrix, which means the coupling between the linear and angular velocities, and describes how changes in the AUV's motion affect the forces and moments that arise from its acceleration or change in direction; $D(v)$ is the damping matrix, which represents the AUV's resistance to the linear and angular motion due to fluid damping forces, where X_u, Y_v, N_r are linear drag coefficients, and D_u, D_v, D_r are the quadratic drag coefficients; $g(\eta)$ is the restoring forces which refer to the forces that act on the vehicle to bring it back to a stable or equilibrium position due to external disturbances or changes in its orientation, $g(\eta) = 0$; τ is the generalized thrust forces and moments, which consists of F_u, F_v, F_r; w is the disturbances vector, including the Indonesian marine conditions, which consists of w_x, w_y, w_z; v is the velocity vector, and for this case encloses only the surge, sway, and yaw motions; and η is the position and orientation vector, includes the position and heading of the vehicle.

Each parameter in Eq. (1) regarding the characteristics of the Cubic Symmetrical AUV model, which was studied by Shen [25], is expressed in:

$$M = \begin{bmatrix} M_{\dot{u}} & 0 & 0 \\ 0 & M_{\dot{v}} & 0 \\ 0 & 0 & M_{\dot{r}} \end{bmatrix}, \tag{2}$$

$$C(v) = \begin{bmatrix} 0 & 0 & -M_{\dot{v}}v \\ 0 & 0 & M_{\dot{u}}u \\ M_{\dot{v}}v & M_{\dot{u}}u & 0 \end{bmatrix}, \qquad (3)$$

$$D(v) = \begin{bmatrix} X_u + D_u|u| & 0 & 0 \\ 0 & Y_v + D_v|v| & 0 \\ 0 & 0 & N_r + D_r|r| \end{bmatrix}, \qquad (4)$$

$$\tau = \begin{bmatrix} F_u \\ F_v \\ F_r \end{bmatrix}, \qquad (5)$$

$$w = \begin{bmatrix} w_u \\ w_v \\ w_r \end{bmatrix}, \qquad (6)$$

$$v = \begin{bmatrix} u \\ v \\ r \end{bmatrix}, \text{ and} \qquad (7)$$

$$\eta = \begin{bmatrix} x \\ y \\ \psi \end{bmatrix}. \qquad (8)$$

Table 1. Hydrodynamic coefficient summary for cubic symmetrical AUV model

No.	Term	Value	Unit
1	$M_{\dot{u}}$	283.6	kg
2	$M_{\dot{v}}$	593.2	kg
3	$M_{\dot{r}}$	29.0	kgm^2
4	X_u	26.9	kg/s
5	Y_v	35.8	kg/s
6	N_r	3.5	kgm^2/s
7	D_u	241.3	kg/m
8	D_v	503.8	kg/m
9	D_r	76.9	kgm^2
10	m	12.0	kg

The authors are breaking Eq. (1) into individual components and considering Eqs. (2)-(8), we obtain the following set of equations of motions of the Cubic Symmetrical AUV model given in Eqs. (9)-(11). Table 1 presents the hydrodynamic coefficients for the Falcon model, categorized as the Cubic Symmetrical AUV model, derived from prior modeling experiments [26].

$$\dot{u} = \frac{M_{\dot{v}}}{M_{\dot{u}}}vr - \frac{X_u}{M_{\dot{u}}}u - \frac{D_u}{M_{\dot{u}}}u|u| + \frac{F_u}{M_{\dot{u}}} - w_x, \qquad (9)$$

$$\dot{v} = -\frac{M_{\dot{u}}}{M_{\dot{v}}}ur - \frac{Y_v}{M_{\dot{v}}}v - \frac{D_v}{M_{\dot{v}}}v|v| + \frac{F_v}{M_{\dot{v}}}, and \qquad (10)$$

$$\dot{r} = \frac{M_{\dot{u}}-M_{\dot{v}}}{M_{\dot{r}}}uv - \frac{N_r}{M_{\dot{r}}}r - \frac{D_r}{M_{\dot{r}}}r|r| + \frac{F_r}{M_{\dot{r}}}. \qquad (11)$$

2.2 Torpedo-like AUV model

The chosen torpedo-like AUV model used in this paper is based on the model by Wahed and Arshad [20], as shown in Figure 2. Similar to the previous Cubic Symmetrical AUV model, the equations of motions of the Torpedo-Like AUV model regarding its characteristics, which have already been studied in references [15, 21, 22], are expressed in Eqs. (12)-(14), where m is the rigid body mass of the Torpedo-Like AUV model; X_u and Y_v are the added mass derivative for surge and sway motion; D_u, D_v, D_r are the hydrodynamic drag

for surge, sway, and yaw motion; I_z is the rigid body inertia in z-axis; F_u, F_v are thrust forces and moment in surge and sway motion; and M_r is the yawing moment due to the thrusters. Table 2 presents the hydrodynamic coefficients for the Torpedo-Like AUV model, obtained from a previous series of modeling experiments performed by references [15, 27].

$$\dot{u} = -\frac{X_u}{m}u - \frac{D_u u^2}{m} + \frac{F_u}{m} - w_x, \qquad (12)$$

$$\dot{v} = -\frac{Y_v}{m}v - \frac{D_v v^2}{m} + \frac{F_v}{m}, and \qquad (13)$$

$$\dot{r} = -\frac{D_r}{I_z}r + \frac{M_r}{I_z}. \qquad (14)$$
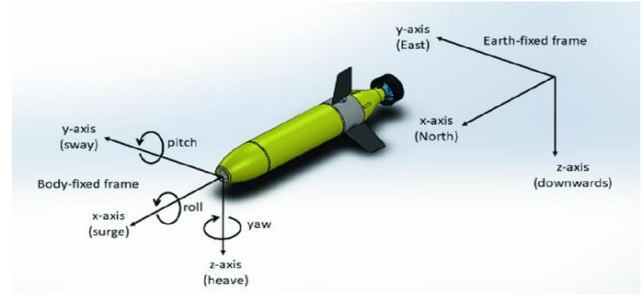
Figure 2. Physical model and the reference frames for the torpedo-like AUV model

Table 2. Hydrodynamic coefficient summary for torpedo-like AUV model

No	Term	Value	Unit
1	X_u	-0.93	kg/s
2	Y_v	-0.35	kg/s
3	D_u	-1.62	kg/m
4	D_v	-1.31	kg/m
5	D_r	-9.40	kgm^2
6	m	14.56	kg
7	I_z	12.02	kgm^2
8	M_r	4.47	kgm^2

3. INDONESIAN SEA CHARACTERISTICS

3.1 The data of Indonesian ocean waves height, period, and wave length

The study [7] yielded valuable information on the characteristics of 15 Indonesian seas, encompassing parameters such as average wave height, wave period, and wavelength. The wave data utilized in the study [7] originates from the authoritative Indonesian government, namely the Indonesian Meteorology, Climatology, and Geophysics Agency (BMKG) [28]. The BMKG acquires information regarding the wave height, duration, and wavelength of sea waves in Indonesian waters through various measurement and surveillance techniques deployed at multiple points along the Indonesian coastline. These methods involve using various tools and resources, including buoys and marine monitoring instruments, coastal monitoring stations, radar, and satellite technology [29].

The Indonesian Sea data obtained by Anggraini et al. [7] spanned one week from June. 7 to June. 14, 2015. Although the results obtained are temporally constrained, they still hold relevance as representative indicators of the Indonesian seas'

characteristics. Within the sample of 30 seas investigated, this study focused on a select group of five well-known oceans for further analysis. The chosen seas encompass the Java Sea, Sulawesi Sea, Bali Sea, Flores Sea, and Arafura Sea, and each property is given in Tables 3 and 4.

3.2 The wave equations of each Indonesian sea characteristics

Derived from the fundamental wave equation formula,

$$y(x,t) = A \sin(kx - \omega t) \tag{15}$$

where,

$k = \frac{2\pi}{\lambda}$, $\omega = 2\pi f$, and $f = \frac{1}{T}$.

We have:

$$y(x,t) = A \sin\left[\frac{2\pi}{\lambda} x - 2\pi f t\right]; y(x,t) = A \sin\left[\frac{2\pi x}{\lambda} - \frac{2\pi t}{T}\right]$$

$$y(x,t) = A \sin\left[2\pi\left(\frac{x}{\lambda} - \frac{t}{T}\right)\right] \tag{16}$$

Eq. (16) uses data from Table 3 for Indonesian seas, and the wave equation from Eq. (15). Table 5 shows the specific characteristics of each sea in Indonesia under maximum (Max) conditions based on Tables 3 and 4, with sea locations depicted in Figure 3.

Table 3. The Indonesian water characteristics (average significant height)

No.	Location	Average Significant Height (A)	
		Min	Max
1	Java sea	0.75m	2.00m
2	Sulawesi sea	0.50m	1.30m
3	Bali sea	0.75m	1.50m
4	Flores sea	1.00m	2.00m
5	Arafura sea	1.50m	3.00m

Table 4. The Indonesian water characteristics (period and wavelength)

No.	Location	Period (T)		Wave Length (λ)	
		Min	Max	Min	Max
1	Java sea	3.07s	5.02s	48.39m	129.00m
2	Sulawesi sea	2.51s	3.97s	32.26m	80.66m
3	Bali sea	3.07s	4.35s	48.39m	96.79m
4	Flores sea	3.55s	5.02s	64.52m	129.00m
5	Arafura sea	4.35s	6.15s	96.79m	193.60m

Table 5. The wave function corresponding to each Indonesian sea

No.	Location	Wave Function
1	Java sea (JS)	$y_{JS} = 2 \sin\left[2\pi\left(\frac{x}{129} - \frac{t}{5.02}\right)\right]$
2	Sulawesi sea (SS)	$y_{SS} = 1.3 \sin\left[2\pi\left(\frac{x}{80.66} - \frac{t}{3.97}\right)\right]$
3	Bali sea (BS)	$y_{BS} = 1.5 \sin\left[2\pi\left(\frac{x}{96.79} - \frac{t}{4.35}\right)\right]$
4	Flores sea (FS)	$y_{BS} = 1.5 \sin\left[2\pi\left(\frac{x}{96.79} - \frac{t}{4.35}\right)\right]$
5	Arafura sea (AS)	$y_{AS} = 3 \sin\left[2\pi\left(\frac{x}{193.6} - \frac{t}{6.15}\right)\right]$
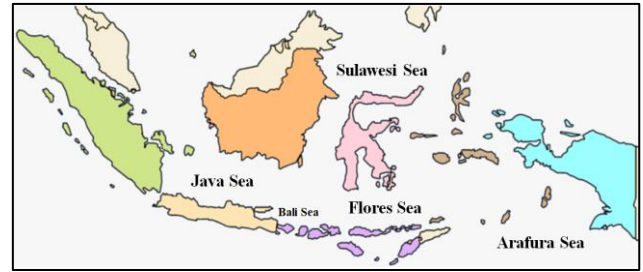
Figure 3. Indonesian map with the corresponding seas

4. SIMULATION RESULTS

Regarding Figure 4, numerical simulation starts with the initial position of AUV at (0, 0, 0) and aims to reach the reference positions (x_d, y_d, z_d). These inputs are channeled into the AUV dynamic model via a pre-established control algorithm. This algorithm processes the inputs mathematically to formulate control laws for the AUV's dynamic model, aligning it with the specified reference position. Alongside the control laws within the AUV dynamic model, a disturbance model represents Indonesian sea conditions. Subsequently, the disparity between the AUV's actual and reference positions (error) is incorporated as feedback within the control algorithm.

The modeling process utilized the ode45 function from the MATLAB library in this particular instance. This function facilitated the resolution of differential equations representing the entire system, including the AUV and environmental models. This simulation aimed to reconstruct each AUV model's performance based on their respective dynamic equations for 90 seconds. In addition, the simulation incorporated the consideration of external disturbances in the form of sea model characteristics, intending to examine each AUV model's response. The comprehensive block diagram of the system for both AUV models can be seen in Figure 3.
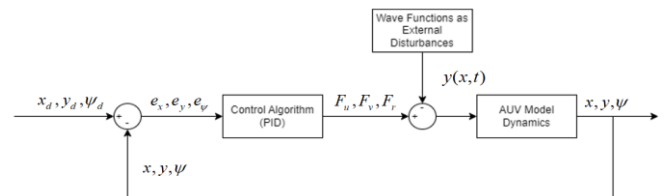
Figure 4. Block diagram system for both torpedo-like and cubic symmetrical AUV models

4.1 Control strategy of AUV motion control

In this modeling approach, the utilized control algorithm is the proportional-integral-derivative (PID) control algorithm, which addresses the error between the desired value (reference) and the actual output obtained from each AUV model. The PID control algorithm aims to minimize the error positions between the reference and the actual output of each AUV model.

Based on Figure 3, the control algorithm F_u, F_v, F_r are expanded for both the AUV model. For the Cubic Symmetrical AUV model, the control inputs are considered as F_{uc}, F_{vc}, and F_{rc}. On the other hand, the Torpedo-Like AUV relies only on two control inputs, such as F_{ut} and F_{vt}. The mathematical models for the control algorithm corresponding to Cubic

Symmetrical AUV inputs are provided by Eqs. (17)-(19), as well as the control algorithm corresponding to Torpedo-Like AUV inputs, are provided by Eqs. (20)-(21).

$$F_{uc} = K_p e_{xc} + K_i \int e_{xc} dt + K_d \left(\frac{de_{xc}}{dt}\right), \qquad (17)$$

$$F_{vc} = K_p e_{yc} + K_i \int e_{yc} dt + K_d \left(\frac{de_{yc}}{dt}\right), \qquad (18)$$

$$F_{rc} = K_p e_{\psi c} + K_i \int e_{\psi c} dt + K_d \left(\frac{de_{\psi c}}{dt}\right), \qquad (19)$$

$$F_{ut} = K_p e_{xt} + K_i \int e_{xt} dt + K_d \left(\frac{de_{xt}}{dt}\right), \qquad (20)$$

$$F_{vt} = K_p e_{yt} + K_i \int e_{yt} dt + K_d \left(\frac{de_{yt}}{dt}\right). \qquad (21)$$

where, $K_p = 150$, $K_i = 1$, and $K_d = 50$ are the best values of PID gain constants obtained by trial and errors. Subsequently, those gain constants are set as control variables for both AUV models; e_{xc}, e_{yc}, and $e_{\psi c}$ are the position errors x, y, and ψ for the Cubic Symmetrical AUV outputs e_{yt} are the position errors x and y Torpedo-like AUV outputs. It is important to note that the control inputs provided to both AUV models represent the total forces acting on each outer side of the AUV rather than being representative of the thruster models. It is because the purpose of this paper is to investigate the performance characteristics of the two different AUV models when encountering Indonesian sea conditions.

The numerical simulation applied dynamic equations from both AUV models to Indonesian sea models represented by different wave equations. These sea models influenced each AUV model's dynamics, impacting their performance output. We assessed their respective performances by comparing the responses of the two AUV models to other Indonesian sea characteristics. The following section presents the results of the conducted numerical simulations.

4.2 Performance of both AUV models in Indonesian waters

This section presents simulation results. Figure 5 displays 3D plots depicting the performance of each AUV physical model in various Indonesian seas. These 3D models help visualize AUV movement underwater. Initially, each AUV starts at the coordinates (0, 0, 0) on the seabed and follows the provided reference position (blue line) to the final coordinate (-19.55, 4.99, -19.55). Further analysis of these results is presented in the following section. In addition to the 3D plots, Figure 6 provides 2D plots for a closer examination of each AUV's performance along the given track reference under diverse sea conditions, allowing for quantitative analysis. Detailed explanations and discussions of these simulation results will follow in the subsequent section.

In addition, besides qualitatively assessing, we conducted quantitative analysis by calculating the Root Mean Square Error (RMSE) for the actual positions relative to reference positions. RMSE measures differences between data sets or models, indicating prediction accuracy, highlighting disparities between tested and reference data, and gauging model quality. RMSE is frequently used for model and algorithm comparisons and can be a data quality control tool. Lower RMSE values signify better agreement between the data or model and reference data. The RMSE results for each

AUV model are presented in Tables 6 and 7, with further elaboration in the following section.
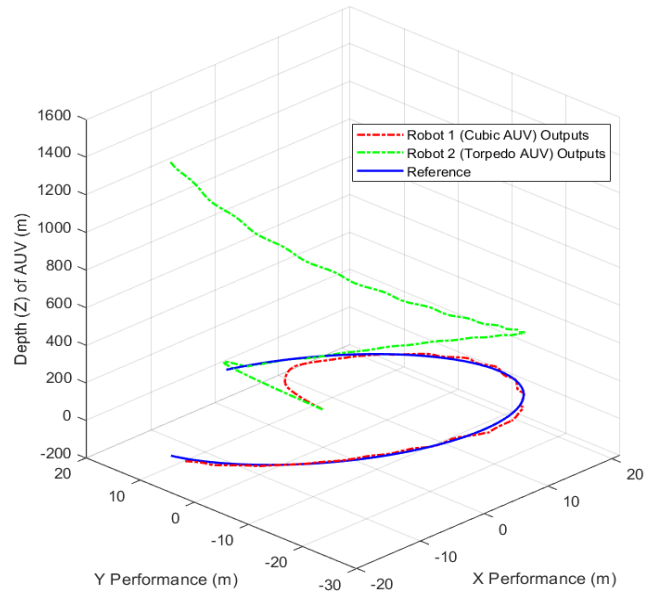
(a) Java sea
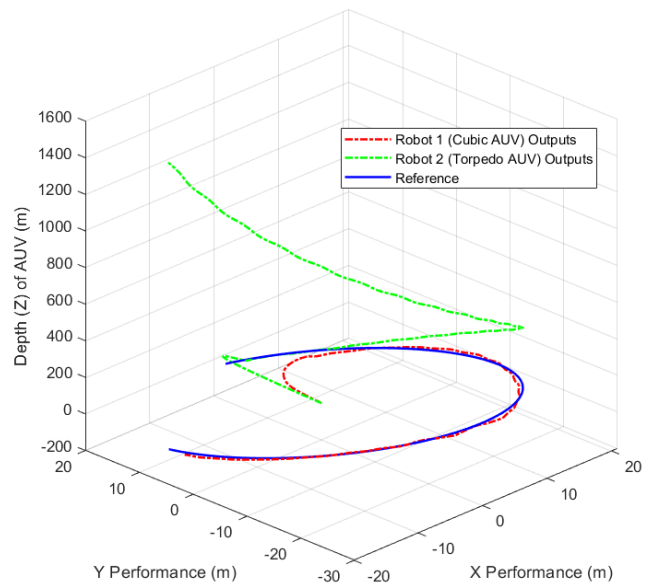
(b) Sulawesi sea
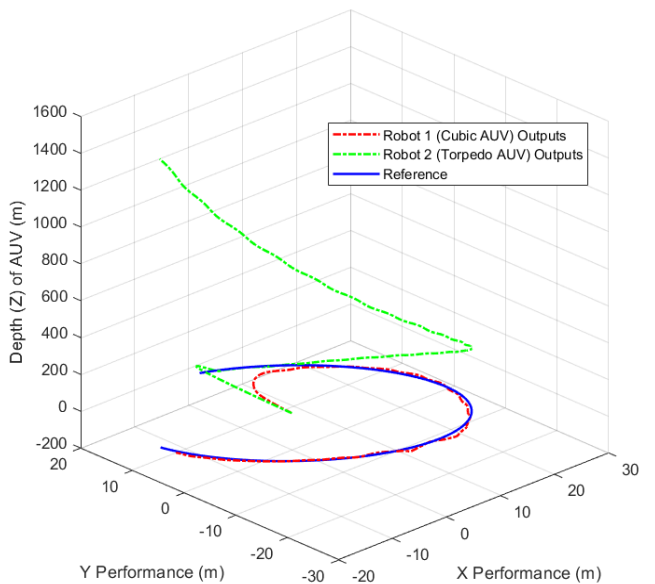
(c) Bali sea

(d) Flores sea

(b) Sulawesi sea
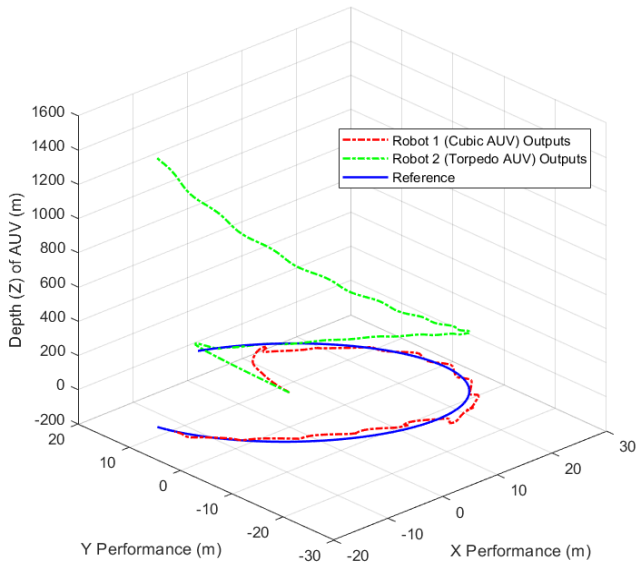
(e) Arafura sea

(c) Bali sea

Figure 5. Three-dimension (3D) AUV performances in Indonesian waters environment
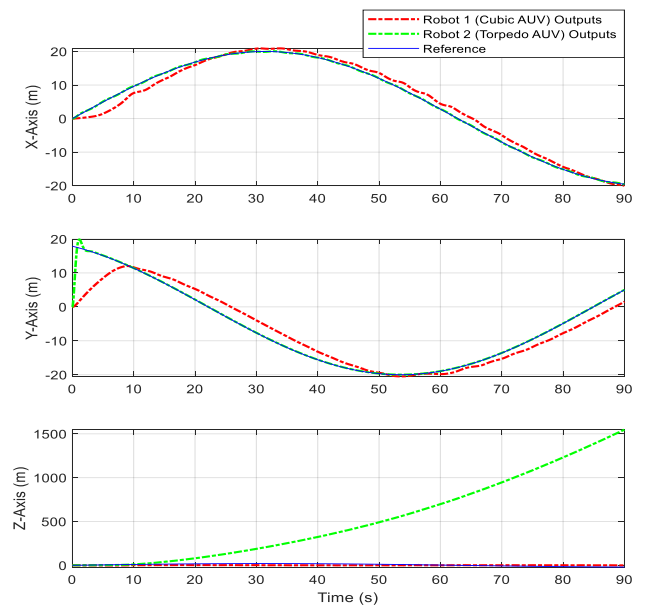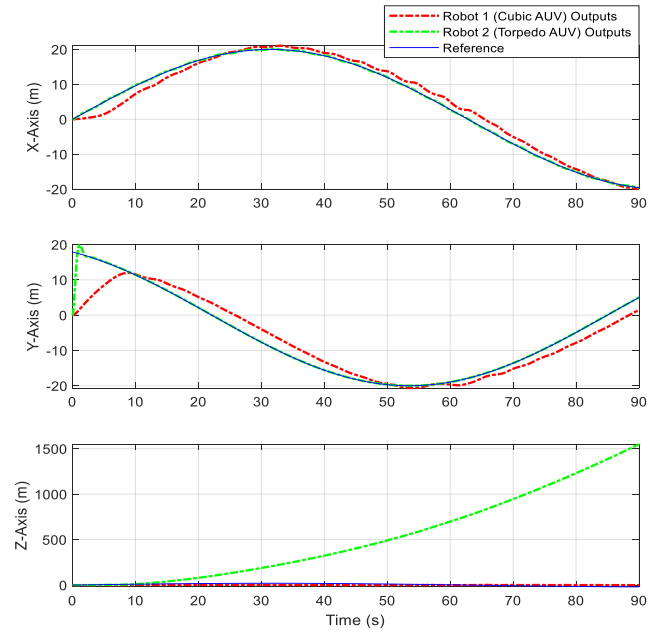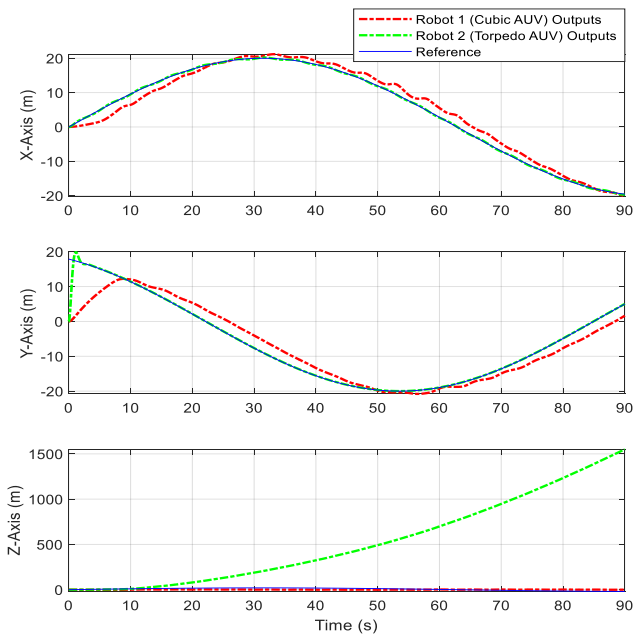
(a) Java sea
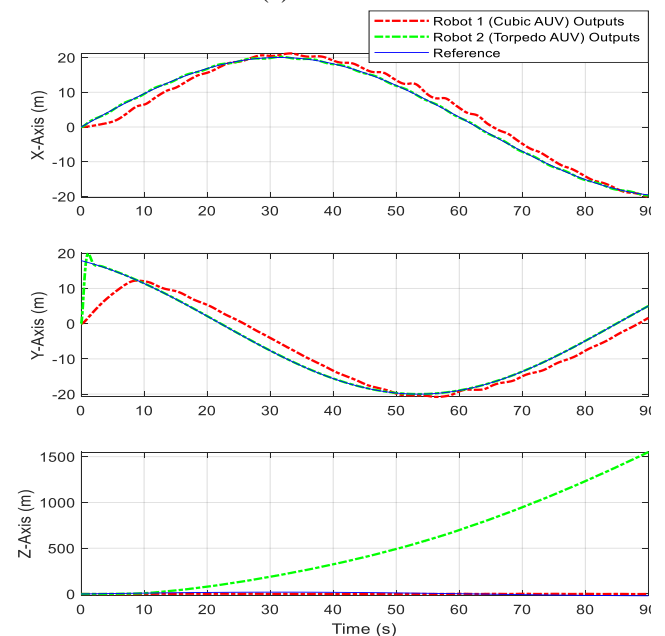
(d) Flores sea
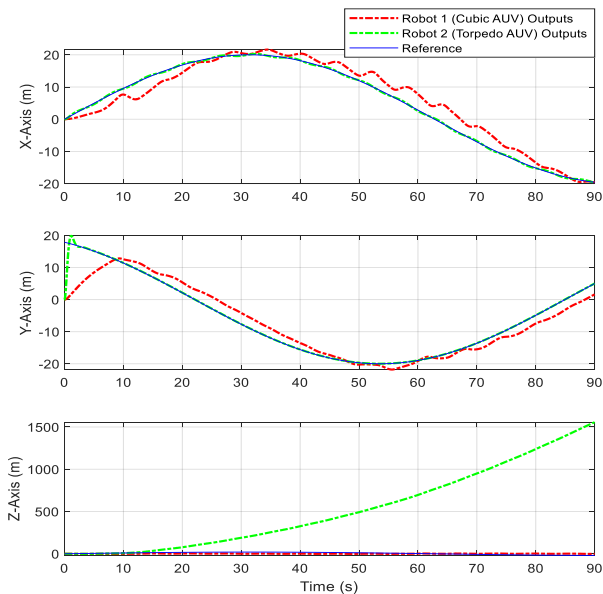
(e) Arafura sea

Figure 6. Two-dimension (2D) AUV performances in Indonesian waters environment

Table 6. The Root Mean Square Error (RMSE) values of the cubic symmetrical AUV performance

No.	Location	Cubic Symmetrical AUV Model RMSE Values		
		x	y	z
1	Java sea	1.87	5.23	13.04
2	Sulawesi sea	1.58	5.41	13.20
3	Bali sea	1.65	5.37	13.18
4	Flores sea	1.87	5.23	13.04
5	Arafura sea	2.86	4.86	11.56

Table 7. The Root Mean Square Error (RMSE) values of the torpedo-like AUV performance

No.	Location	Torpedo-Like AUV Model RMSE Values		
		x	y	z
1	Java sea	0.14	2.98	680.66
2	Sulawesi sea	0.10	3.02	683.09
3	Bali sea	0.11	3.02	685.13
4	Flores sea	0.14	2.98	680.66
5	Arafura sea	0.19	2.85	503.94

5. DISCUSSIONS AND ANALYSIS

In underwater missions, the torpedo and symmetrical cubic models are commonly used for robots or vehicles. This study examines these two models explicitly and does not consider biomimetic characteristics resembling underwater creatures.

The primary focus of this study lies in determining the optimal vehicle model. The decision regarding the chosen model is based on specific requirements, including the anticipated underwater environmental conditions, the mission objectives, and the relevant design capabilities. This study aims to discuss selecting the most suitable vehicle model for executing underwater missions in the Indonesian Seas, considering relevant characteristics. The authors utilize the findings in reference [7] on characterizing sea waves in various Indonesian regions to represent disturbance models in the conducted model simulations. Quantitative data on the sea wave characteristics are presented in Table 3, necessitating a conversion into the general wave equation and selecting the maximum value (Table 3 and Table 4). These results of wave equations represent external disturbances of the Indonesian waters that AUV encountered. Assuming the AUV traverses in the opposite direction to the external disturbance, a negative (-) value is assigned to the external disturbance models.

Simulations were conducted for five specific sea locations: the Java Sea, Sulawesi Sea, Bali Sea, Flores Sea, and Arafura Sea. MATLAB's ode45 solver was employed for numerical simulation in solving differential equation problems. The outcomes of these simulations were represented in a 3D plot in Figure 5, which illustrates the positional performance of each AUV model in the presence of an external disturbance.

Figure 5 (a) describes the AUV model navigating the underwater conditions of the Java Sea. The blue line represents the reference trajectory, the red line represents the movement of the cubic symmetrical AUV model, and the green line represents the movement of the torpedo-like AUV model. Figure 5 (a) illustrates that Robot 1, represented as the AUV symmetrical cube model, can approach the desired endpoint of (-19.55, 4.99, -19.55) closely as it reaches the final coordinates of (-20.18, 1.63, 0.16). On the other hand, Robot 2, resembling a torpedo-like model, reaches its final position at (-19.72, 5.02, 1550.58). It indicates that the cubic symmetrical AUV performs better in trajectory tracking than the torpedo-like model in the Java Sea characteristics, especially in the vertical axes. Similar results are observed for the remaining sea models, as illustrated in Figures 5 (b-e). This disparity arises due to the differential actuation capabilities of the cubic symmetrical AUV model compared to the torpedo-like AUV model. Unlike the cubic symmetrical subic AUV model, which possesses actuators for all axes, the torpedo-like AUV model only relies on a single actuator in the tail (Figure 2), limiting its ability to perform outside horizontal movements.

Furthermore, the authors evaluate the robustness of each AUV model in the presence of external disturbances by analyzing the positional performance of each AUV from a two-dimensional perspective, as presented in Figure 6. Figure 6 (a) illustrates the two-dimensional positional performance of the two AUV models in the Java Sea in three axes, X, Y, and Z axes, versus time in seconds. The torpedo-like AUV model performs better in handling external disturbances than the cubic symmetrical AUV, as evidenced by minimal oscillations regarding the reference line. This trend is observed across other underwater conditions, as shown in Figures 6 (b-e).

Due to its streamlined and hydrodynamic shape, the torpedo-like AUV is better equipped to handle disturbances than the cubic symmetrical AUV model [30]. This streamlined design reduces hydrodynamic drag and turbulence, allowing the torpedo-like AUV to move through the water more efficiently. Additionally, the torpedo-like shape minimizes the impact of cross currents and waves because it offers less surface area for these forces to act upon. It also provides excellent stability, as its design inherently resists rolling and pitching motions in response to external disturbances. In contrast, with its box-like shape, the cubic symmetrical AUV model presents a larger frontal area to water flow and is more prone to drag and turbulence. It also lacks the inherent stability of the torpedo-like shape, making it less capable of maintaining steady movement in the presence of disturbances.

Moreover, quantitative validation was conducted by

calculating the Root Mean Square Error (RMSE) to assess both AUV models' performance regarding the reference path in Tables 5 and 6. Table 5 shows the RMSE values for the cubic symmetrical AUV model in the Java Sea, with values of 1.87, 5.23, and 13.04 for the x, y, and z coordinates. In contrast, Table 6 displays the RMSE values for the torpedo-like AUV model, which are 0.14, 2.98, and 680.66 for the x, y, and z coordinates, respectively. It suggests that the torpedo-like AUV performs better in handling sea waves, especially in x and axes. However, it is worth noting that this advantage does not extend to the z-axis, as the RMSE value for the torpedo-like AUV model dramatically exceeds that of the symmetrical cubic AUV model. This discrepancy arises due to the inherent inability of the torpedo-like AUV model to achieve vertical control, resulting in inferior performance along the vertical axis when compared to the symmetrical cubic AUV model. These observations align with results obtained under varying sea conditions, including the Sulawesi, Bali, Flores, and Arafura Sea.

The AUV torpedo model and the symmetrical cubic shape exhibit distinct advantages and disadvantages. Due to its superior hydrodynamic characteristics, the torpedo model outperforms the symmetrical cubic AUV in handling sea waves. However, the torpedo model's vertical control limitations pose a significant drawback, particularly in precision-demanding underwater exploration missions. Its hydrodynamic nature makes the torpedo-like AUV model highly suitable for high-speed underwater operations, such as military and defense applications, for example, the HUGIN model employed by the Royal Norwegian Navy (RNoN) [31], as well as the commercial use, for instance, Sparus II AUV for seabed inspection [32]. In contrast to the torpedo-like AUV, the cubic symmetrical AUV lacks hydrodynamic abilities. Nevertheless, due to its control system characteristics, the cubic symmetrical AUV can be maneuvered in multiple directions and equipped with various sensors for conducting exploration tasks. As a result, the cubic symmetrical AUV, which prioritized maneuverability over speed, is highly advisable for underwater missions like exploration or mapping [33].

Both AUVs, characterized by their hydrodynamic design, find diverse applications in the commercial sector beyond military and exploration. They prove indispensable in underwater archaeology for documenting shipwrecks and ancient sites without disturbing fragile relics. The oil and gas industry inspects pipelines to prevent leaks and structural issues. Environmental consulting firms use them for impact assessments, while salvage companies rely on their locating capabilities. They're also vital in deep-sea mining maritime security and offer unique underwater tourism experiences. In media, they capture stunning footage for documentaries and movies. Their efficiency in navigating challenging underwater environments makes them valuable assets across various commercial industries [34].

This research comes with several noteworthy limitations. To start, Indonesia's ever-changing seas, driven by shifts in natural conditions, pose the primary challenge. Consequently, further research and ongoing monitoring are imperative to delve deeper into these fluctuations. Additionally, within the applied model, Indonesia's sea characteristics incorporated as external disturbances do not comprehensively address the y and z axes, calling for further refinement. Lastly, the study exclusively focuses on wave models as disturbances, disregarding static or dynamic physical obstacles.

Furthermore, additional methodologies are required to accurately model these variables to understand Indonesia's marine environment comprehensively. Asumsi gangguan static [35].

6. CONCLUSIONS

This study aims to evaluate the performance of two physical autonomous underwater vehicle (AUV) models in various sea conditions in Indonesia: a cubic symmetrical AUV and a torpedo-like AUV. Wave data from various Indonesian seas was employed as external factors affecting each AUV. The study involved numerical simulations using MATLAB's ode45 solver to assess the performance of both AUV designs. The results of the simulations revealed that the cube-shaped symmetrical AUV displayed superior trajectory tracking accuracy compared to the torpedo-shaped AUV when considering coordinate reference. Conversely, the torpedo-shaped AUV demonstrated better resilience in dealing with external disturbances from a two-dimensional perspective, albeit with slightly reduced coordinate accuracy.

The cubic symmetrical AUV demonstrates exceptional trajectory tracking accuracy, making it highly suitable for various underwater tasks. It excels in surveying and mapping applications, enabling the creation of detailed underwater maps for scientific research, archaeology, and environmental monitoring. Additionally, its precision is valuable for precise infrastructure inspection and efficient search and rescue operations, aiding in locating specific objects or locations like shipwrecks and lost equipment. Scientific research contributes to collecting high-quality data, particularly for tracking underwater species and studying ecosystems. On the other hand, the torpedo-like AUV's resilience against external disturbances positions it as the ideal choice for high-speed exploration missions, allowing for swift coverage of vast ocean areas in oceanographic studies or marine resource exploration. Its disturbance-handling capability is advantageous in underwater surveillance, where rapid responses and adaptability are critical, enabling monitoring of underwater structures and detecting unauthorized activities. In dynamic environments, such as tracking underwater currents and monitoring pollutant spread, the torpedo-like AUV's agility in handling disturbances provides real-time and dynamic data for effective environmental monitoring.

For further research, it's crucial to incorporate comprehensive real-time Indonesian marine data encompassing all axes (x, y, and z) rather than solely the x-axis. This approach will yield more precise performance results, providing a more representative evaluation of the two AUV models in Indonesian waters. Furthermore, we should also account for dynamic obstacles in simulation, utilizing improved methods like software-in-the-loop (SITL), hardware-in-the-loop (HITL), or even real-world implementation.

resources and financial support, which was essential for completing this research.

REFERENCES

[1] Fadhiil, M.D., Afriansyah, A. (2022). Strategic development of Indonesia's outermost islands as an enhancement of national maritime defense and sovereignty. Udayana Journal of Law and Culture, 6(1): 83-107. https://doi.org/10.24843/UJLC.2022.v06.i01.p05

[2] Camila, T.R., Saraswati, R. (2020). Vulnerability of the East Coast of Balikpapan City in East Kalimantan (Lamaru Beach-Klandasan Beach). In IOP Conference Series: Earth and Environmental Science, Central Java Province, Indonesia, IOP Publishing, 448(1): 012128. https://doi.org/10.1088/1755-1315/448/1/012128

[3] Kurniawan, R., Khotimah, M.K. (2016). Ocean wave characteristics in Indonesian waters for sea transportation safety and planning. IPTEK The Journal for Technology and Science, 26(1): 19-27. https://doi.org/10.12962/j20882033.v26i1.767

[4] Rizal, A.M., Ningsih, N.S. (2022). Description and variation of ocean wave energy in Indonesian seas and adjacent waters. Ocean Engineering, 251: 111086. https://doi.org/10.1016/j.oceaneng.2022.111086

[5] Rachmayani, R., Ningsih, N.S., Ramadhan, H., Nurfitri, S. (2018). Analysis of ocean wave characteristic in Western Indonesian Seas using wave spectrum model. The Third International Conference on Sustainable Infrastructure and Built Environment (SIBE 2017). https://doi.org/10.1051/matecconf/201814705001

[6] Rachmayani, R., Ningsih, N.S., Ramadhan, H., Nurfitri, S. (2018). Analysis of ocean wave characteristic in Western Indonesian Seas using wave spectrum model. In MATEC Web of Conferences, EDP Sciences, 147: 05001. https://doi.org/10.1051/matecconf/201814705001

[7] Anggraini, D., Al Hafiz, M.I., Derian, A.F., Alfi, Y. (2015). Quantitative analysis of Indonesian Ocean wave energy potential using oscillating water column energy converter. MATTER: International Journal of Science and Technology, 1(1): 228-239. https://doi.org/10.20319/mijst.2016.s11.228239

[8] Bernardi, M., Hosking, B., Petrioli, C., Bett, B.J., Jones, D., Huvenne, V.A., Marlow, R., Furlong, M., McPhail, S., Munafò, A. (2022). AURORA, a multi-sensor dataset for robotic ocean exploration. The International Journal of Robotics Research, 41(5): 461-469. https://doi.org/10.1177/02783649221078612

[9] Klischies, M., Rothenbeck, M., Steinführer, A., Yeo, I.A., dos Santos Ferreira, C., Mohrmann, J., Faber, C., Schirnick, C. (2018). AUV abyss workflow: autonomous deep sea exploration for ocean research. In 2018 IEEE/OES Autonomous Underwater Vehicle Workshop (AUV), IEEE, 1-6. https://doi.org/10.1109/AUV.2018.8729722

[10] Ratnasari, Y., Pandewo, A.F., Santoso, S.A., Anas, D.F., Lestari, N.A., Iqbal, M., Jaya, I. (2020). N3-AUV (nusantara 3-autonomous underwater vehicle): Design and implementation for underwater exploration. In IOP Conference Series: Earth and Environmental Science, IOP Publishing, 429(1): 012038. https://doi.org/10.1088/1755-1315/429/1/012038

[11] Di Ciaccio, F., Troisi, S. (2021). Monitoring marine environments with autonomous underwater vehicles: A bibliometric analysis. Results in Engineering, 9: 100205. https://doi.org/10.1016/j.rineng.2021.100205

[12] Moline, M.A., Blackwell, S.M., von Alt, C., Allen, B., Austin, T., Case, J., Forrester, N., Goldsborough, R., Purcell, M., Stokey, R. (2005). Remote environmental monitoring units: An autonomous vehicle for characterizing coastal environments. Journal of Atmospheric and Oceanic Technology, 22(11): 1797-1808. https://doi.org/10.1175/JTECH1809.1

[13] Gutnik, Y., Avni, A., Treibitz, T., Groper, M. (2022). On the adaptation of an auv into a dedicated platform for close range imaging survey missions. Journal of Marine Science and Engineering, 10(7): 974. https://doi.org/10.3390/jmse10070974

[14] Yang, Y., Xiao, Y., Li, T.S. (2021). A survey of autonomous underwater vehicle formation: performance, formation control, and communication capability. IEEE Communications Surveys & Tutorials, 23(2): 815-841. https://doi.org/10.1109/COMST.2021.3059998

[15] Chen, Y.Y., Lee, C.Y., Huang, Y.X., Yu, T.T. (2022). Control allocation design for torpedo-like underwater vehicles with multiple actuators. In Actuators, MDPI, 11(4): 104. https://doi.org/10.3390/act11040104

[16] Wu, C.J. (2018). 6-Dof modelling and control of a remotely operated vehicle. Flinders University, College of Science and Engineering.

[17] Bu, K.L., Gong, X.B., Yu, C.L., Xie, F. (2022). Biomimetic aquatic robots based on fluid-driven actuators: A review. Journal of Marine Science and Engineering, 10(6): 735. https://doi.org/10.3390/jmse10060735

[18] Li, Q., Cao, Y., Li, B.Y., Ingram, D.M., Kiprakis, A. (2020). Numerical modelling and experimental testing of the hydrodynamic characteristics for an open-frame remotely operated vehicle. Journal of Marine Science and Engineering, 8(9): 688. https://doi.org/10.3390/JMSE8090688

[19] Einarsson, E.M., Lipenitis, A. (2020). Model predictive control for the BlueROV2 theory and implementation. Master's Thesis, Aalborg University. https://www.et.aau.dk/.

[20] Wahed, M.A., Arshad, M.R. (2019). Modeling of torpedo-shaped micro autonomous underwater vehicle. In 10th International Conference on Robotics, Vision, Signal Processing and Power Applications: Enabling Research and Innovation Towards Sustainability, Springer Singapore, 457-463. https://doi.org/10.1007/978-981-13-6447-1_58

[21] Helgason, B., Leifsson, L., Rikhardsson, I., Thorgilsson, H., Koziel, S. (2012). Low-speed modeling and simulation of torpedo-shaped AUVs. In International Conference on Informatics in Control, Automation and Robotics, SCITEPRESS, 2: 333-338. https://doi.org/10.5220/0004047103330338

[22] Zhao, B.W., Sun, J.Y., Zhang, D.P., Zhu, K.Q., Jiang, H.Y. (2023). Dynamic analysis of underwater torpedo during straight-line navigation. Applied Sciences, 13(7): 4169. https://doi.org/10.3390/app13074169

[23] BlueRobotics. (2023). https://bluerobotics.com/.

[24] Fossen, T.I. (2011). Handbook of Marine Craft Hydrodynamics and Motion Control. John Wiley & Sons.

[25] Shen, C. (2018). Motion control of autonomous underwater vehicles using advanced model predictive control strategy. University of Victoria.

[26] Proctor, A.A. (2014). Semi-autonomous guidance and control of a saab seaeye falcon ROV. University of Victoria.

[27] Prestero, T. (2001). Verification of a six-degree of freedom simulation model for the REMUS autonomous underwater vehicle. Massachusetts Institute of Technology (MIT).

[28] Badan Meteorologi, Klimatologi, dan Geofisika. https://www.bmkg.go.id/.

[29] Sprintall, J., Gordon, A.L., Wijffels, S.E., Feng, M., Hu, S.J., Koch-Larrouy, A., Phillips, H., Nugroho, D., Napitu, A., Pujiana, K., Susanto, R.D., Sloyan, B., Peña-Molino, B., Yuan, D.L., Riama, N.F., Siswanto, S., Kuswardani, A., Arifin, Z., Wahyudi, A.J., Zhou, H., Nagai, T., Ansong, J.K., Bourdalle-Badié, R., Chanut, J., Lyard, F., Arbic, B.K., Ramdhani, A., Setiawan, A. (2019). Detecting change in the Indonesian seas. Frontiers in Marine Science, 6. https://doi.org/10.3389/fmars.2019.00257

[30] Tian, W.L., Song, B.W., Ding, H. (2019). Numerical research on the influence of surface waves on the hydrodynamic performance of an AUV. Ocean Engineering, 183: 40-56.

https://doi.org/10.1016/j.oceaneng.2019.04.007

[31] Hagen, P.E., Storkersen, N., Marthinsen, B.E., Sten, G., Vestgard, K. (2005). Military operations with HUGIN AUVs: Lessons learned and the way ahead. In Europe Oceans, IEEE, 2: 810-813. https://doi.org/10.1109/OCEANSE.2005.1513160

[32] Carreras, M., Hernández, J.D., Vidal, E., Palomeras, N., Ribas, D., Ridao, P. (2018). Sparus II AUV-a hovering vehicle for seabed inspection. IEEE Journal of Oceanic Engineering, 43(2): 344-355. https://doi.org/10.1109/JOE.2018.2792278

[33] Willners, J.S., Carreno, Y., Xu, S.D., Łuczyński, T., Katagiri, S., Roe, J., Pairet, È., Petillot, Y., Wang, S. (2021). Robust underwater slam using autonomous relocalisation. IFAC-PapersOnLine, 54(16): 273-280. https://doi.org/10.1016/j.ifacol.2021.10.104

[34] Chapariha, M. (2022). Systems dynamics model of SDGs: A case study of Iran. Challenges in Sustainability, 10(1): 3-22. https://doi.org/10.12924/cis2022.10010003

[35] Sahoo, A.K., Chakraverty, S. (2023). Modeling of Mexican Hat Wavelet Neural Network with L-BFGS algorithm for simulating the recycling procedure of waste plastic in ocean. Journal of Engineering Management and Systems Engineering, 2(1): 61-75. https://doi.org/10.56578/jemse020104